FOUNTAIN JOURNAL OF NATURAL & APPLIED SCIENCES

A Publication of the College of Natural & Applied Sciences

Fountain University, Osogbo, Nigeria

Reservoir-scale petrographic and grain size study of Bida basin sandstones: A geophysical perspective on porosity and depositional trends

Issa, T. A.[1,2*], Olatunji, S.[1]

[1]*Department of Geophysics, Faculty of Physical Sciences, University of Ilorin, Ilorin, Nigeria.*
[2]*Department of Geology and Mineral Science, Faculty of Pure and Applied Sciences, Kwara State University, Malete, Nigeria.*

**Correspondence:* taofeeq.issa@kwasu.edu.ng

ABSTRACT

This study investigated the granulometric and petrographic characteristics of siliciclastic sediments in parts of the Northern Bida Basin, with the aim of evaluating their influence on porosity, permeability, and hydrocarbon storage potential through aeromagnetic and sedimentological analyses The objectives are to: (i) determine area of low magnetic intensity, (ii) determine the grain size distribution, (iii) assess petrographic features, (iv) determine the heavy mineral composition, and (v) delineate the possible areas for good porosity and permeability. The study revealed that: (i) the sandstones are characterized by coarse to very coarse grains, with moderate to poor sorting, and exhibit a very leptokurtic distribution, indicating a good reservoir quality due to high porosity and permeability; (ii) the bivariate plots reveals that the sediments are primarily of fluvial and beach origin; (iii) the petrographic analysis indicates dominance of quartz amongst the constituents, which reflects a mature sediment source; (iv) the sediment exhibits a mixed origin; and (v) Kutigi and Bida locations appear to have the best potential for hydrocarbon storage due to their better sorting and grain distribution, leading to improved permeability. The study concluded that the Bida Basin showed hydrocarbons with key petroleum elements, though immature source rocks limit generation. The study, therefore, recommended detailed characterisation of petroleum system elements and reservoir quantification for further studies to achieve a comprehensive hydrocarbon prospectivity of the basin.

ARTICLE INFO

Article history:
Received July 2025
Revised September 2025
Accepted September 2025

Keywords:
Grain size analysis, Bida Basin, porosity, petrography, heavy mineral analysis, hydrocarbon reservoir.

Introduction

Grain size is an important physical property of sediments and is vital for our understanding of intrinsic properties and dynamic forces that operate during deposition. Moreover, grain-size parameters help probe the depositional environment and the energy flux of the agents that transported the sediments. The last century witnessed remarkable advances in grain-size analysis as a tool for deducing the provenance of sediment, transport pathways, sedimentary processes, and depositional environments [1-11]. Certain restrictions, such as diagenetic changes and subsequent modifications that framework particles undergo in clastic deposits, are recognised alongside the depositional environment and the operational mechanisms of ancient sedimentation [7]. Grain-size characteristics have been effectively employed in prior research to provide important insights into provenance, transit method, and depositional environment, despite these limitations [12-15]. Furthermore, because they depend more on the processes that were in place when the sediments were deposited, these parameters, such as sedimentary structures and their associations, palaeocurrent, geometry, and fossil content, need to be studied in conjunction with grain size analysis to gain a better understanding of depositional environments [16].

Geology of the study area

Previous reports of changes in lithostratigraphy have been controversial. In the entire Bida basin, the

DOI: https://doi.org/10.53704/fujnas.v14i2.970

Upper Cretaceous layers were referred to as the Lokoja Series by [17] in his seminal work, while [18] called them the Nupe Group. The northern and southern sediments of the Bida Basins were separated by [19]. The Patti and Campanian-Maastrichtian Lokoja Formations make up those in the southern Bida Basin. The Agbaja Ironstone Formation is the successor of the Patti Formation, according to [20]. These are lateral equivalents of the Bida Formation, Sakpe Ironstone, Enagi Silstone, and Batati Ironstone in the northern part of the basin. These successions together form lateral equivalents of the Campanian to Maastrichtian Mamu, Ajali, and Nsukka Formations. In the adjacent Anambra Basin, a major depocenter in the Lower Benue Trough during the post-Santonian sedimentation (Fig. 1). It should be noted that some authors [21-22] did not recognise the lithostratigraphic differentiations of [19] and described the entire Campanian to Maastrichtian sediments in the southern Bida Basin as the Lokoja Sandstone. In the current study and recent ones [23-24], the authors uphold the subdivision into distinct mappable stratigraphic units in southern Bida, as per [19, 25]. Overlying the Precambrian to lower Palaeozoic Crystalline Basement rocks is the non-conformable base Lokoja Formation. It is exposed mainly between Lokoja and Kotonkarfi. The lithologic units in this formation range from conglomerates and sandstones to claystones. They are thought to have been deposited on alluvial fans in shallow marine environments [23]. The Maastrichtian Patti Formation (Fig. 1), which is visible on the Agbaja Plateau and north of Kotonkarfi, overlies the Lokoja Formation. The Patti Formation has two distinct members: sandstone and shale-claystone. For the sandstone and shale-claystone components, [21] proposed a Maastrichtian date, whereas [25] proposed a Campanian to Maastrichtian age.

[26] regarded the shale-claystone section as nonmarine swamp sediments, whereas a meandering river model was proposed by [25] for the Patti deposits. Based on the presence of dinoflagellate assemblages including Deflandrea, Dinogymnium, and Spiniferites, recent paleoecologic studies by [23] Ojo & Akande (2006) demonstrate that the basal section of the shale-claystone component indicates a period of shallow sea flooding during the Maastrichtian.

According to [27-28], the oolitic and concretional ironstone facies that make up the Agbaja Formation, the uppermost lithostratigraphic unit, are directly overlain by the Patti Formation on the Agbaja Plateau. The ironstones were formed by minor marine reworking of some primary kaolinitic clay particles.

Methods

Six sheets of airborne magnetic data used for this study were acquired from the Nigerian Geological Survey Agency. This data was part of the dataset acquired during a nationwide airborne survey between 2005 and 2009 by Fugro Airborne Survey, which was supervised by the agency. The six aeromagnetic data sheets acquired are 182 (Mokwa), 183 (Egbako), 184 (Bida), 203 (Lafiagi), 204 (Pategi), and 205 (Baro), which correspond to the area covered by latitude 8^0 30^1 N to 9^0 30^1 N and longitude 5^0 00^1 E to 6^0 00^1 E. Each 1:100,000 topographical sheet covers an area of about 3025 km^2 (i.e., 55 km x 55 km), totalling a superficial area of 18,150 km^2. Following the integration of the six data sheets to produce the Total Magnetic Intensity (TMI) map, areas exhibiting low magnetic intensity were selected for granulometric and petrographic analyses (Fig. 2a).

As a consequence of the sketch of the character of each outcrop, the logging of bed characteristics was done. Fifty-four (54) samples coined as (RAB-4, ENA-15, KUT-8, DOK-13, BID-10 & BIDD-4) were collected for granulometric analysis from six different locations within the northern Bida Basin (Figs. 1& 2b). For granulometric analysis, a Ro-tap shaker was used in conjunction with mechanical sieving. For 10 minutes, 100 g of each sample was sieved through a series of sieves with mesh sizes of 2360, 1180, 850, 425, 300, 150, 75, and 63 microns. Weighing and recording the fractions of the particle grains that were kept in the base pan and each sieve. Cumulative mass percentages were then calculated. The results of the granulometric study were used to create statistical plots, including cumulative frequency and frequency curves on a log-probability graph. The intercepts of the cumulative frequency curves (i.e. plots of grain size versus cumulative mass retained) at the 5th, 16th, 25th, 50th, 75th, 84th, and 95th percentiles were obtained and were employed to determine textural parameters such as the graphic mean particle size (M), inclusive standard deviation (sorting) (r), graphic kurtosis (KG) and inclusive graphic skewness (SK) for each sample. The average for each size parameter was determined using the formulae proposed by Folk & Ward (1957) [1].

Bivariate plots (Fig. 5) were widely used to express relationships among several statistical variables and to infer the environmental conditions at the time of

DOI: https://doi.org/10.53704/fujnas.v14i2.970

sediment deposition. These bivariate plots, which combine grain-size parameters, have been used to discriminate among depositional environments.

Twenty-seven from different locations (RAB-(3), ENA-(5), KUT-(4), DOK-(6), BID-(4), and BIDD-(5) sandstone samples were prepared for thin section, and they were studied under transmitted polarizing microscope and percentage of the different constituent was obtained (Table 4.3). The framework components of the studied sandstone are quartz and feldspar grains, accessory minerals, and metamorphic, sedimentary, and igneous fragments.

Heavy minerals are a very important group of minerals that exist in clastic sedimentary rocks because they are provenance indicators. The general properties of heavy minerals are divided into two types: opaque and nonopaque minerals. 18 samples were used in this study to identify and count heavy minerals in the sandstones of the Kutigi and Bida sections.

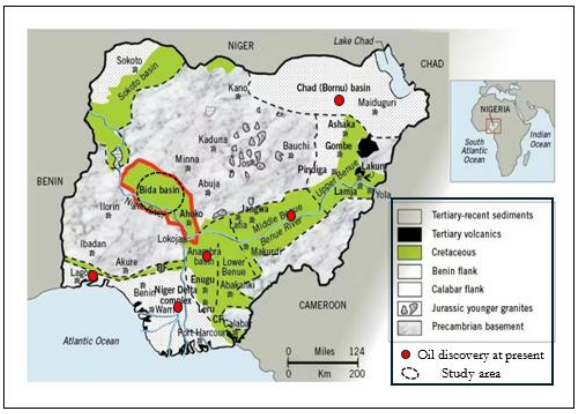

Fig.1: Map of Nigeria showing the different sedimentary basins, oil discovery, and study area [30]

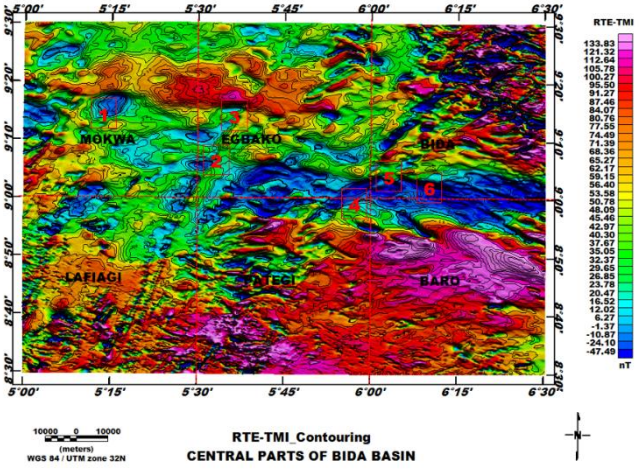

Fig. 2a: Sample locations from magnetic intensity map (LOC1-RAB, LOC2-ENA, LOC3- KUT, LOC4-DOK, LOC5-BID & LOC6-BIDD)

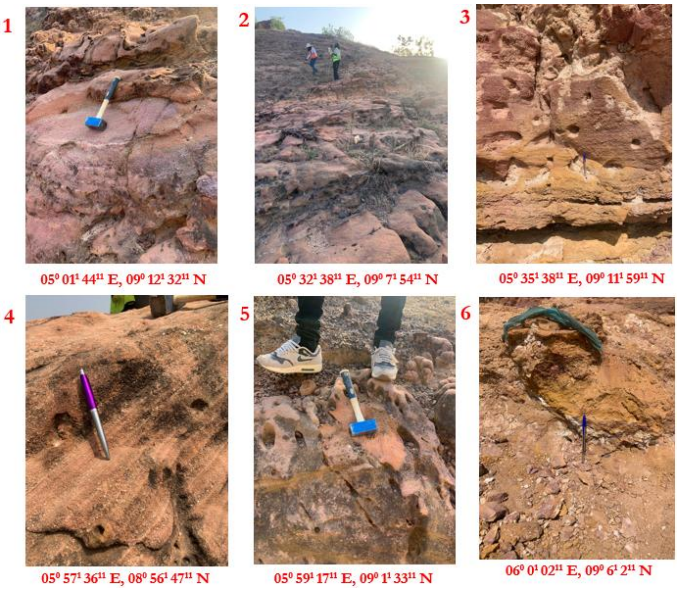

Fig 2b: Sample locations (LOC1-RAB, LOC2-ENA, LOC3-KUT, LOC4-DOK, LOC5-BID & LOC6-BIDD)

Results and interpretation

Aeromagnetic data analysis

The Total Magnetic Intensity (TMI) map (Fig. 2a) reveals alternating zones of strong and weak magnetic anomalies, indicative of variations in the magnetisation of the underlying basement rocks across the study area. These anomalies are categorised as high (red), low (blue), and intermediate (yellow to green), exhibiting predominant structural trends in NE–SW, NW–SE, N–S, WNW–ESE, and E–W directions. High magnetic anomalies, ranging from 77.5 to 133.8 nT, are mainly concentrated in the southeastern and eastern regions of the map. In contrast, low anomalies, between –47.49 and 12.02 nT, are prominent in the central area and scattered across other parts of the basin. The northern section is largely characterised by intermediate anomalies, ranging from 20.47 to 70.5 nT. Overall, the magnetic signatures observed in the area exhibit distinct, varying amplitudes and dimensions, with trends that align closely with the basin's structural orientation. Areas of low magnetic susceptibility is an indication of areas purely of sedimentary cover.

Granulometric analysis of sampled sediments

Granulometric analysis of selected samples (Fig. 2) was conducted to provide additional information on depositional processes and environments, thereby reinforcing the earlier inferences drawn from the

DOI: https://doi.org/10.53704/fujnas.v14i2.970

lithofacies association and sedimentary structures in the sections studied.

Frequency curves

The phi values are plotted against cumulative frequencies, pointing to different modes of sediment transport and deposition and their importance in the genesis of sandstone units. The curve usually shows an S-shaped trend when plotted on an arithmetic scale (Fig. 3). Sorting can be predicted by the slope of the middle portion of the curve. A gentle, broad slope indicates low velocity and kinetic energy, resulting in poor sorting. In contrast, a very steep slope indicates good sorting. The cumulative frequencies range from 0 to 100, and the phi values range from -3.0 to 5.0. The samples are mostly very coarse-grained, and a few are medium-coarse-grained. Hence, they can safely be assigned to the medium- to coarse-grained category. The steepness of the slope shows that these grains are very well sorted to moderately sorted.

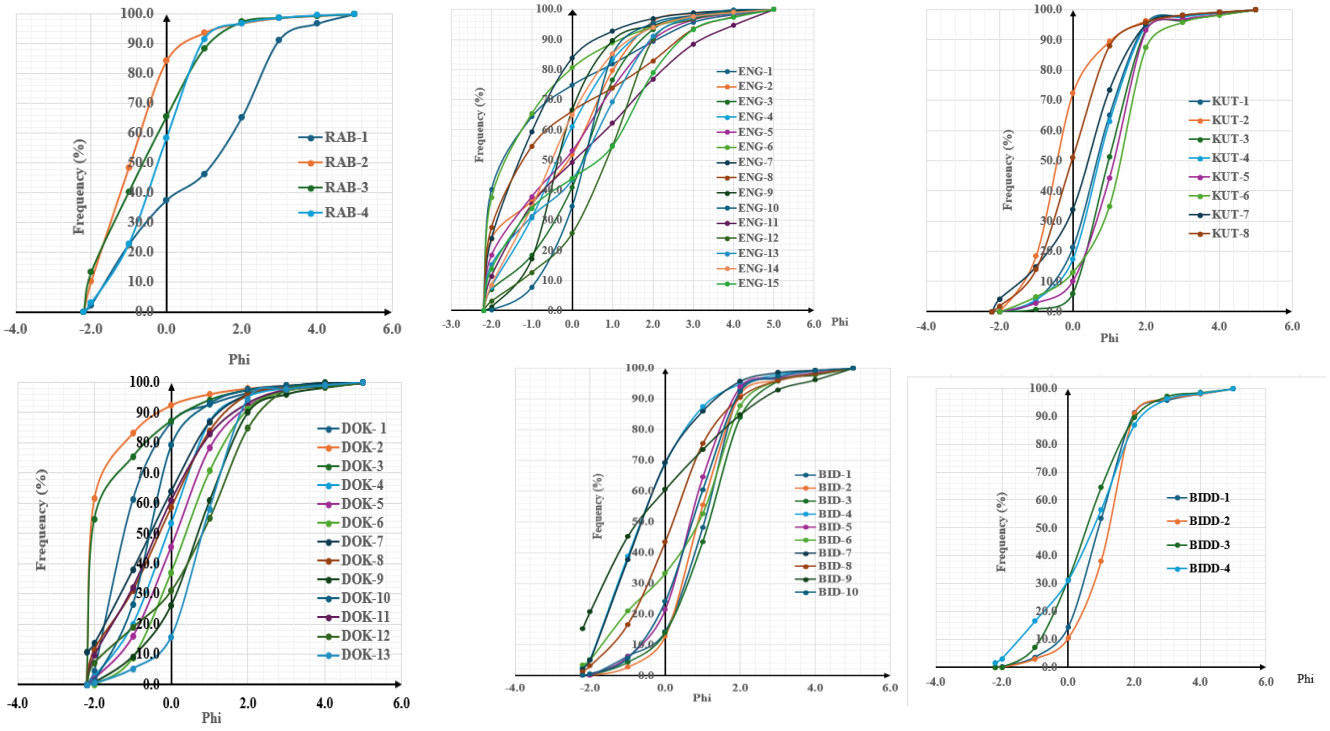

Fig 3: Cumulative frequency curve for RAB, ENA, KUT, DOK, BID, and BIDD for grain size distribution.

Statistical parameters- Graphical method

1. Inclusive graphic median (Φ50): Graphic median denotes that at the value of Φ50, half of the particles distribution and 41.5% coarser grain size distribution. This indicates that the area consists of a mix of grains.

2. Graphic mean size (M): This depicts the average particle size or the central tendency of particles. The graphic mean ranges from -1.76 to 1.10, with an average of 0.071; negative values indicate coarser grains from high-energy environments (e.g., rivers or dunes), and positive values indicate finer grains from low-energy environments (e.g., marine settings). (Tables 1a & b).

3. Standard Deviation-Sorting (r): This measures the sorting or uniformity of the grains, indicating energy conditions that prevailed during transport and deposition. It ranges from 0.68 to 2.06, with an average are coarser, and the other half finer. The values in our samples range from -2.18 to 1.30 Φ, with an average of 0.070 Φ (Tables 1a & b). It has 58.5% finer grain size of 1.18; most samples show moderate sorting (1.0 to 1.5), indicating mixed energy conditions. Well-sorted sediments (below 1.0) are associated with stable environments like beaches, whereas poorly sorted sediments (above 1.5) indicate variable-energy environments such as rivers or deltas (Tables 1a & b).

4. Graphic skewness (SK): This measures the degree of asymmetry in the frequency curves in terms of the predominance of fine- or coarse-grained fractions. The skewness values in our samples range from -7.0ϕ to 14.09ϕ, with an average of 0.85ϕ. Negative skewness indicates a distribution toward coarser grains, typical of high-energy environments like rivers or coastal dunes (Tables 1a & b).

DOI: https://doi.org/10.53704/fujnas.v14i2.970

Table 1a: Multivariate analysis of grain size parameters in the northern Bida basin sandstones.

SN	Samples	Sorting (r)	Mean (M)	Skewness(SK)	Kurtosis (KG)
1	RAB-1	1.79	0.87	-4.60	7.03
2	RAB-2	0.93	-0.93	1.78	2.49
3	RAB-3	1.25	-0.57	1.28	3.11
4	RAB-4	0.98	-0.30	0.00	1.57
5	ENA-1	1.60	-0.89	14.09	4.30
6	ENA-2	1.47	-0.36	-1.52	3.34
7	ENA-3	1.24	0.17	-1.74	2.75
8	ENA-4	1.27	-0.33	1.70	2.86
9	ENA-5	1.65	-0.23	1.74	5.51
10	ENA-6	1.26	-1.20	8.60	2.75
11	ENA-7	1.09	-1.16	3.69	1.17
12	ENA-8	1.88	-0.43	13.70	6.95
13	ENA-9	0.99	-0.3	2.24	1.67
14	ENA-10	0.85	0.23	0.13	1.34
15	ENA-11	2.06	0.23	7.16	8.64
16	ENA-12	1.26	0.67	-3.82	2.75
17	ENA-13	1.39	0.24	-1.19	5.09
18	ENA-14	1.30	-0.43	2.20	3.00
19	ENA-15	1.85	0.37	-3.43	7.17
20	KUT-1	0.86	0.67	-0.55	1.42
21	KUT-2	0.88	-0.33	1.44	1.31
22	KUT-3	0.68	1.00	0.00	0.90
23	KUT-4	0.86	0.73	-0.35	1.43
24	KUT-5	0.79	1.00	-0.74	1.08
25	KUT-6	1.01	1.10	-2.21	1.52
26	KUT-7	1.17	0.30	-1.71	2.40
27	KUT-8	0.97	-0.03	0.86	1.81

Table 1b: Multivariate analysis of grain size parameters in the northern Bida basin sandstones.

SN	Samples	Sorting (r)	Mean (M)	Skewness (SK)	Kurtosis (KG)
28	DOK-1	1.02	-0.93	3.86	3.09
29	DOK-2	0.76	-1.76	4.97	0.71
30	DOK-3	1.13	-1.33	7.99	1.61
31	DOK-4	1.10	-0.07	-0.91	2.18
32	DOK-5	1.13	0.07	0.70	2.46
33	DOK-6	1.11	0.43	0.64	2.30
34	DOK-7	1.30	-0.17	-7.00	3.19
35	DOK-8	1.32	-0.4	1.03	3.36
36	DOK-9	1.24	0.63	-0.66	2.58
37	DOK-10	0.83	-0.57	0.98	1.11
38	DOK-11	1.38	-0.33	2.32	3.50
39	DOK-12	1.36	0.23	-4.82	4.02
40	DOK-13	0.87	0.80	-1.09	1.40
41	BID-1	0.92	0.96	-1.92	1.60
42	BID-2	0.82	0.90	0.00	1.23
43	BID-3	1.05	1.10	-0.99	2.12
44	BID-4	0.95	-0.51	3.74	1.53
45	BID-5	0.92	0.67	0.03	1.52
46	BID-6	1.47	0.47	-4.78	1.70
47	BID-7	1.20	-0.07	-4.87	2.59
48	BID-8	1.28	0.20	1.13	2.95
49	BID-9	1.95	-0.37	11.51	7.25
50	BID-10	1.00	0.65	-0.47	1.70
51	BID(2)-1	0.88	0.93	-0.52	1.54
52	BID(2)-2	0.80	1.10	-1.35	1.26
53	BID(2)-3	1.14	0.56	0.19	2.40
54	BID(2)-4	1.43	0.56	-2.38	3.81

DOI: https://doi.org/10.53704/fujnas.v14i2.970

Interrelationship of size parameters

Bivariate plots, in the form of scatter plots between statistical parameters, are drawn to distinguish depositional settings, based on the assumption that they reflect differences in the fluid-flow mechanisms governing sediment transport and deposition [31]. The mean grain-size and sorting plot shows poorly sorted, medium-sand sediments, indicating deposition in moderate-energy environments with variable energy conditions, such as rivers, deltas, beaches, or shallow marine settings (Fig. 4A). Poorly sorted sediments can be attributed to tractive currents in the beach subenvironment. The faster rounding of these sediments is also caused by the continuous back and forth of grains in such a sub-environment [32]. Moderately high-energy depositional conditions are indicated by coarse-grained sediments [33]. The bivariate plot between skewness and mean shows the skewness distribution indicates energy variations, with fine-skewed sediments forming in low-energy conditions and coarse-skewed sediments in high-energy environments (Fig. 4B). Many of them also lie in near symmetrical - very fine-skewed. Mean size vs kurtosis bivariate shows Leptokurtic sediments indicate uniform grain sizes in high-energy conditions, mesokurtic sediments reflect balanced distributions in moderate-energy settings, and the absence of platykurtic sediments suggests minimal highly variable energy conditions (Fig. 4C). Standard deviation vs skewness and standard deviation vs kurtosis show that the moderately sorted sediments are finely skewed, having a mesokurtic, leptokurtic and very leptokurtic (Fig. 4D, E). The skewness vs kurtosis plot shows fine- to very fine-skewed, reflecting the platykurtic to very platykurtic nature of the sediments (Fig. 4F).

Bivariate grain size parameters

Most of the points fall in the river domain (to the right of the coastal dune boundary line). A few points lie near the boundary between coastal dunes and river deposits. This suggests that the sediment samples are predominantly from river environments, but some exhibit characteristics indicative of coastal dune environments. Most of the sediment samples plot in the fluvial domain (right of the marine-fluvial boundary line), indicating a dominance of river deposits.

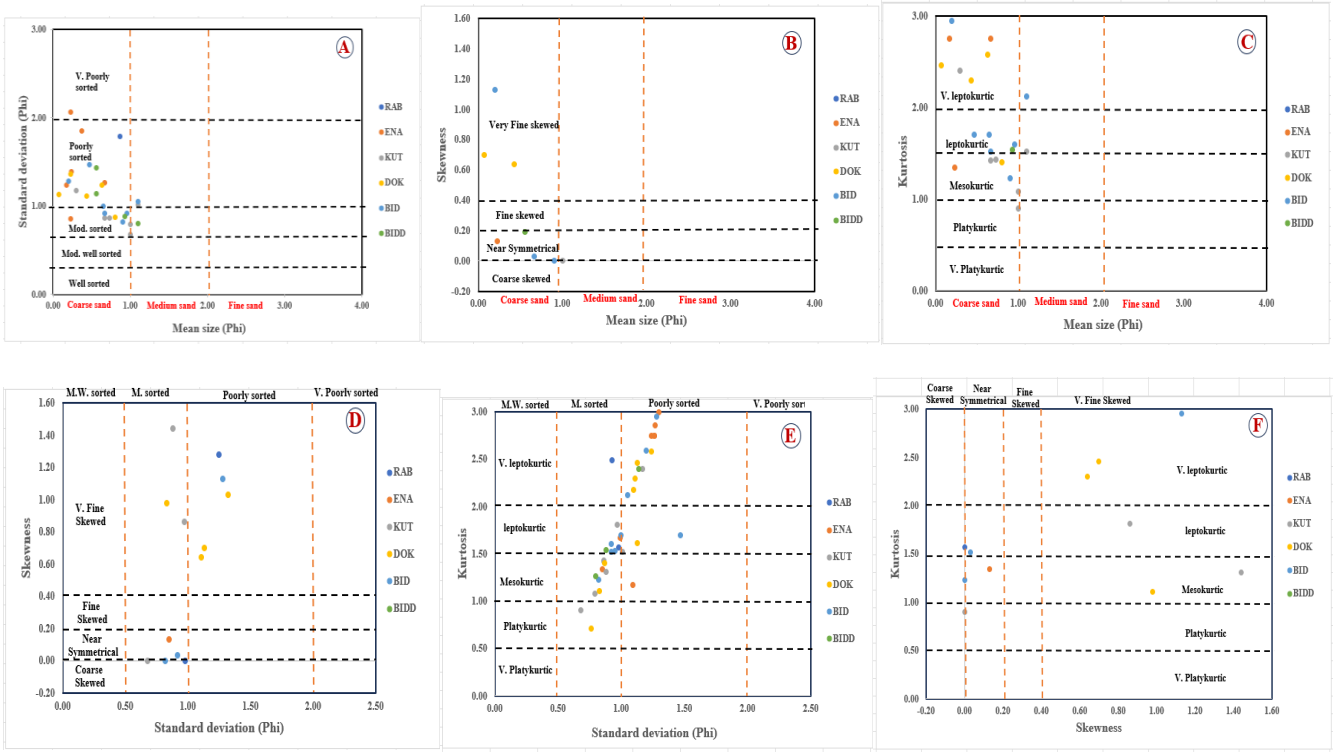

Fig 4: Bivariate relationship between: A – Grain size and sorting; B – Grain size and skewness; C – Grain size and kurtosis; D – Sorting and skewness; E – Sorting and kurtosis; F – Skewness and kurtosis for sediments' textural characteristics.

DOI: https://doi.org/10.53704/fujnas.v14i2.970

Some samples plot near the boundary or slightly within the marine domain, suggesting mixed depositional influences (Fig 5).

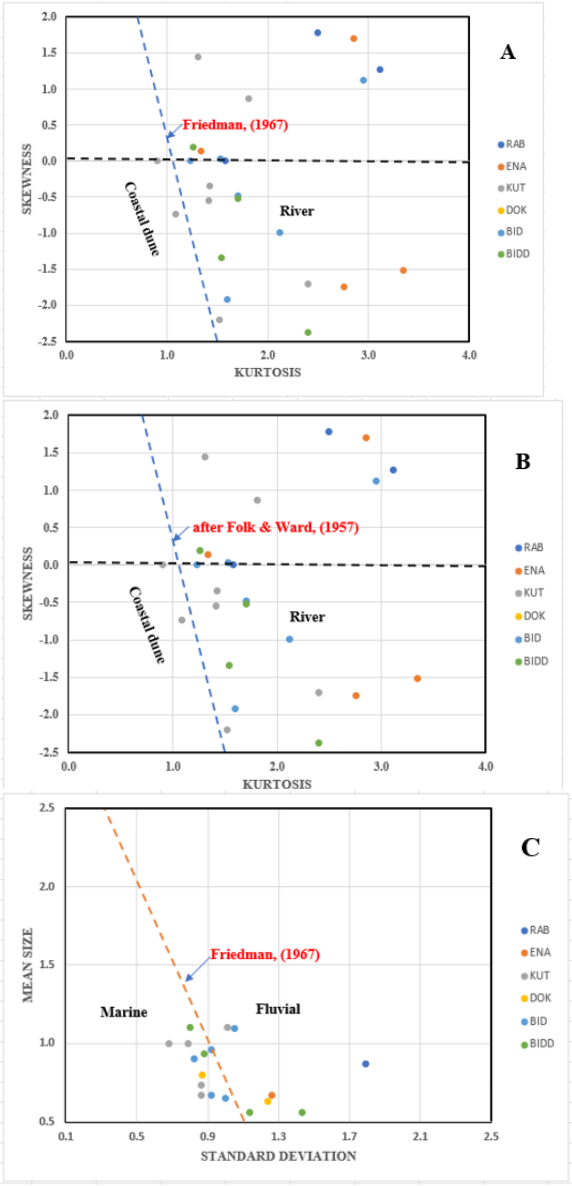

Fig 5: Bivariate plots showing the depositional environments, A – Kurtosis vs Skewness [3], B- Kurtosis vs Skewness [1], and C- Standard deviation vs Mean size [3]

Petrographic analysis

The framework components of the studied sandstone are quartz and feldspar grains, accessory minerals, and metamorphic, sedimentary, and igneous fragments (Fig. 6). Quartz forms the main constituent in the studied sandstones, ranging from 70 % to 92 % with an average of 84.2 % (Table 4.3). Monocrystalline and polycrystalline quartz grains were recognised. Monocrystalline quartz is angular to subrounded, usually showing straight extinction and occasionally wavy extinction, indicating a metamorphic origin [32]. Polycrystalline quartz grains contain aggregates of quartz crystals that are sub-angular to sub-rounded. The amount of polycrystalline quartz is less than that of monocrystalline quartz, which is due to the resistance of the quartz to weathering, while the increasing amount of monocrystalline quartz is due to the localisation of its source rock.

Most of the rock fragments are terrigenous grains derived from older source rocks that survived destruction. They are very important for studying source rocks and are more reliable than individual minerals, such as quartz and feldspar, which can be derived from different source rocks [34]. The total rock fragments are between 1-6 %, averaging 13.1 (Table 4.3). Sedimentary rock fragments are the most abundant lithics, with a small percentage of igneous rock fragments, attributable to igneous source rocks [35].

The matrix represents ligament materials that fill the voids between particles and generally consists of formed clay and micritic materials [36]. It is produced because of the disintegration and decomposition of unstable constituents, especially rock fragments and feldspar. The matrix amount ranges from 9.3-25.6% and averages 17.48% (Table 4.3). The matrix is divided into autochthonous and allochthonous. Autochthonous origin was created by diagenesis, while allochthonous origin was transported from the source area and deposited in the basin [37]. Where the matrix is mainly friable, it is autochthonous [38].

Cement is a binding material deposited from chemical solutions present between grains. The main kinds of cement in the study are iron, and accessory minerals are also present.

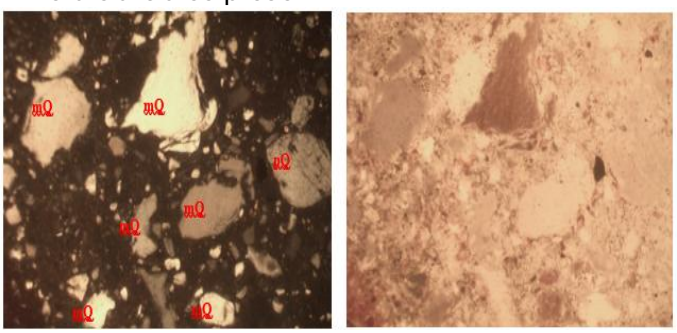

Fig. 6: Thin section photomicrographs for mineral compositions (Q-quartz, OP-opaque mineral, RF-rock fragment)

DOI: https://doi.org/10.53704/fujnas.v14i2.970

Table 2:Recalculated framework composition (%) of the sandstones in parts of the Bida basin.

SN	Sample No.	Quartz (Q)	Feldspar (F)	Lithic Fragment (L)	Q/F+L
1	RB1A	84	10	6	5.25
2	RB1C	90	8	2	9.00
3	RB1D	90	6	4	9.00
4	EN2A	75	24	1	3.00
5	EN2B	82	13	5	4.56
6	EN2F	91	7	2	10.11
7	EN2H	90	6	4	9.00
8	EN2N	70	30	0	2.33
9	KT3A	80	15	5	4.00
10	KT3B	90	10	0	9.00
11	KT3D	90	6	4	9.00
12	KT3G	74	35	1	2.06
13	DK4A	85	10	5	5.67
14	DK4B	85	10	5	5.67
15	DK4E	92	6	2	11.50
16	DK4H	90	6	4	9.00
17	DK4L	74	35	1	2.06
18	DK4N	85	10	5	5.67
19	BD5A	85	10	5	5.67
20	BD5B	92	6	2	11.50
21	BD5C	90	6	4	9.00
22	BD5D	74	35	1	2.06
23	BDD6A	75	20	5	3.00
24	BDD6B	92	6	2	11.50
25	BDD6F	90	6	4	9.00
26	BDD6I	73	26	1	2.70
27	BDD6J	85	10	5	5.67
Minimum		**70.0**	**6.0**	**1.0**	**2.06**
Maximum		**92.0**	**35.0**	**6.0**	**11.50**
Average		**84.2**	**13.8**	**3.1**	**6.50**

This ternary QFL (Quartz-Feldspar-Lithic fragments) diagram (Fig. 7) classifies the sandstone samples by mineral composition. Most samples plot within the Subarkose and Quartzarenite fields, indicating a dominance of quartz with minor feldspar content. A few samples extend into the Lithic Arkose field, showing some feldspar input but minimal lithic fragment presence. The absence of samples in the Litharenite field suggests a limited contribution from lithic fragments. The quartz dominance reflects a mature sediment source, likely of cratonic or recycled orogenic origin, in which prolonged weathering and transport led to feldspar breakdown. Such sediment characteristics point to deposition in stable continental environments, such as beaches, eolian systems, or passive margins, where long-term weathering and sediment recycling are common. The presence of Subarkose and Lithic Arkose hints at limited feldspar input, possibly from granitic or gneissic sources, while the scarcity of lithic fragments suggests low tectonic activity during deposition. Overall, the sandstones reflect a mature, quartz-rich provenance from a tectonically stable source region.

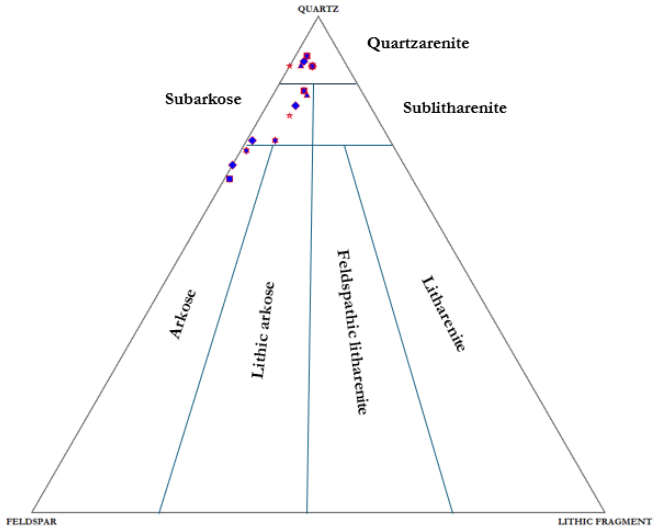

Fig. 7: Ternary Classification of the Rabba, Enagi, Kutigi, Doko, Bida & Bida Sandstones based on framework composition for provenance study

DOI: https://doi.org/10.53704/fujnas.v14i2.970

The QFL ternary diagram of [39], which relates sediment provenance to tectonic environments, was also used to characterise the sediment clasts from the study area. Most of the sample points (RAB, ENA, KUT, DOK, BID, BIDD) fall within or very close to Field 1 – Cratonic Interior (Fig. 8). This field is quartz-rich, indicating high compositional maturity, stable continental source rocks (e.g., older continental cratons), long transport distance or extensive recycling, and low tectonic activity at the source. The samples' placement in the Cratonic Interior field suggests they are quartz-rich, compositionally mature sandstones, likely derived from a stable continental source, making them excellent reservoir candidates in hydrocarbon systems due to their high porosity, chemical stability, and low diagenetic alteration.

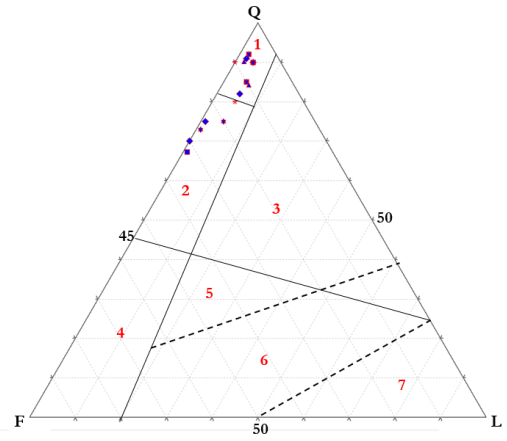

Fig. 8: Ternary diagram of the sandstone clasts showing provenance types in the study area (Modified after [39])

Heavy mineral analysis

The heavy mineral analysis was conducted in two sections to determine the provenance and maturity of the sediments. (Figs. 9 and 13).

Kutigi section

The sandstone samples studied showed that the opaque heavy minerals comprise a higher percentage, averaging 53.87% (Fig. 10). These opaques are usually derived from Mafic igneous rocks [40]. The non-opaque minerals constitute the lowest percentage, averaging 46.13%. (Fig. 10) This group of heavy minerals is usually positively identifiable under the polarising microscope because they can transmit light. These heavy minerals can be classified by stability into three subgroups: ultrastable, metastable, and unstable [32]. The ultrastable heavy minerals include zircon, tourmaline, and rutile. Their Presence is evidence of metamorphic rocks derived from acidic igneous source rocks [41] or from mafic igneous and metamorphic source rocks [42].

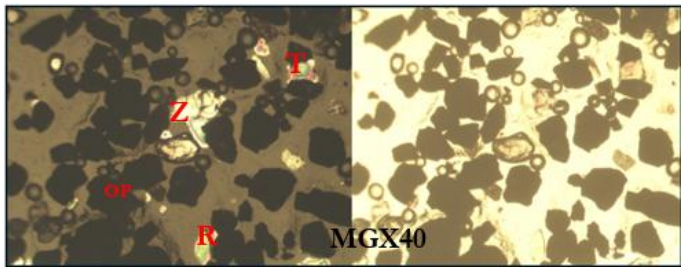

Fig. 9: Thin section photomicrographs for mineral constituents (Z-Zircon, T-Tourmaline & R-Rutile)

Zircon

Zircon is found as subrounded grains or prisms with pyramidal ends. It can be derived from metamorphic and acidic igneous source rocks. The rounded grains are abundant in reworked sediments [43,40]. Zircon is characterised by its colourless, pale yellow, or pale pink colour with high relief. The amount of zircon is between 5.11 - 27.87% (Table 4).

Tourmaline

Tourmaline is a group of minerals with complex chemical compositions and various colours. The variation in colours is due to the complexity of chemical composition, and they all show paleochroism. The subrounded grains are usually brown to yellowish brown, representing derivatives [44]. The percentage ranges from 17.82% to 46.45% (Table 4). It is derived from metamorphic and igneous source rocks, while the rounded grains are derived from reworked sediment sources [43, 40].

Rutile

Rutile can be identified by its high relief, red or brown to yellowish-orange colour, and paleochroism from yellow to reddish brown [43] (Kern, 1959). The rounded grains are derived from reworked sediment sources, while the platy forms are derived from mafic igneous rocks [40]. The rutile content ranges from 7.19% to 37.02% (Table 4).

The 'ZTR' index (Table 3), which is a quantitative definition of the mineral assemblage, was computed using the percentage of the combined zircon, tourmaline, and rutile grains for each sample [45] according to the formula below.

$$ZTR_{index} = \frac{Zircon\% + Tourmaline\% + Rutile\%}{Total\ Transparent\ Heavy\ Minerals} \times 100$$

DOI: https://doi.org/10.53704/fujnas.v14i2.970

The formula is referred to as [45] Scheme. The computed index is expressed as a percentage to ascertain the mineralogical maturity of the sediment. The heavy mineral data from the KUT samples generally reflect a provenance ranging from sub-mature to mature, with some samples displaying super-mature characteristics.

Table 3: ZTR index interpretation, [45] Interpretation [46]

ZTR %	Interpretation
<50	Immature
50 -75	Mature
>75	Super-mature

Table 4: Composition of heavy mineral suites and ZTR indices for Kutigi Formation

Samples	Opaque Minerals	Non-Opaque Minerals					Z %	T %	R %	O %	ZTR index	[45]
		Z	T	R	O	TNOP						
KUT1	384	14	115	39	83	251	5.58	45.82	15.54	33.07	66.93	Mature
KUT2	406	19	98	38	56	211	9.00	46.45	18.01	26.54	73.46	Mature
KUT3	257	21	62	45	93	221	9.50	28.05	20.36	42.08	57.92	Mature
KUT4	234	12	94	87	42	235	5.11	40.00	37.02	17.87	82.13	Super-mature
KUT5	278	24	43	15	112	194	12.37	22.16	7.73	57.73	42.27	Immature
KUT6	186	31	52	24	83	190	16.32	27.37	12.63	43.68	56.32	Mature
KUT7	316	97	62	27	162	348	27.87	17.82	7.76	46.55	53.45	Mature
KUT8	223	73	58	22	153	306	23.86	18.95	7.19	50.00	50.00	Mature

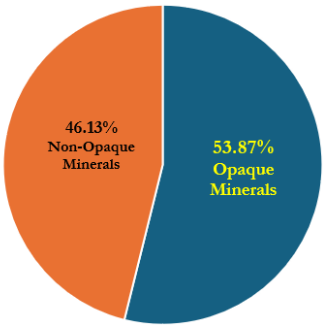

Fig. 10: Pie chart showing percentages of opaque and non-opaque minerals of the studied sandstone

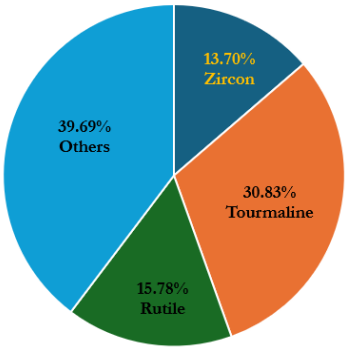

Fig. 11: Pie chart showing the percentage of non-opaque minerals in the studied sandstone

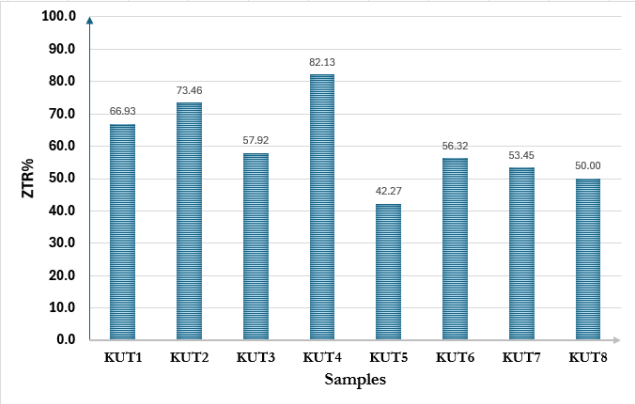

Fig. 12: Bar Chart of ZTR Index of each selected sample of Kutigi sandstone

This elevated level of mineralogical maturity suggests extensive weathering and long-distance sediment transport, likely involving recycling from older sedimentary rocks originally derived from felsic igneous (granitic) and high-grade metamorphic sources. The consistently high proportion of opaque minerals across the samples further indicates efficient hydraulic sorting within the depositional environment.

DOI: https://doi.org/10.53704/fujnas.v14i2.970

Bida section

The sandstone samples studied showed that the opaque heavy minerals comprise a higher percentage, averaging 51.27% (Fig. 14). These opaques are usually derived from Mafic igneous rocks [40]. The non-opaque minerals constitute the lowest percentage, averaging 48.73%. (Fig. 14) This group of heavy minerals is usually positively identifiable under the polarising microscope because they can transmit light. These heavy minerals can be classified by stability into three subgroups: ultrastable, metastable, and unstable. The ultrastable heavy minerals include zircon, tourmaline, and rutile. Their Presence is evidence of metamorphic rocks, which were derived from acidic igneous source rocks [41], or metamorphic and igneous mafic source rocks [42].

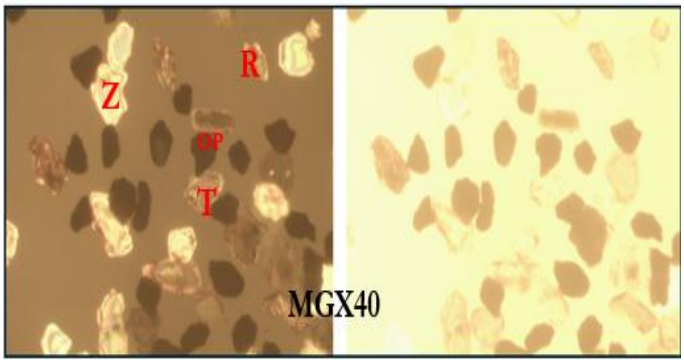

Fig. 13: Thin section photomicrographs (Z-Zircon, T-Tourmaline & R-Rutile))

Zircon

Zircon occurs as subrounded grains or prisms with pyramidal terminations. It can be derived from metamorphic and acidic igneous source rocks. The rounded grains are abundant in reworked sediment [43,40]. Zircon is characterised by its colourless, pale yellow, or pale pink colour with high relief. The amount of zircon is between 4.23 14.97% (Table 5).

Tourmaline

Tourmaline is a group of minerals with complex chemical compositions and various colours. The variation in colours is due to the complexity of chemical composition, and they all show paleochroism. The subrounded grains are usually brown to yellowish brown, representing derivatives [44]. The percentage ranges from 21.62% to 47.26% (Table 5). It is derived from metamorphic and igneous source rocks, while the rounded grains are derived from reworked sediment sources [43, 40].

Rutile

Rutile can be identified by its high relief, red or brown to yellowish-orange colour, and paleochroism from yellow to reddish brown [43]. The rounded grains are derived from reworked sediments [40], while the platy forms are derived from mafic igneous rocks [40]. The rutile content ranges from 8.61% to 31.62% (Table 5).

Table 5: Composition of heavy mineral suites and ZTR indices for Bida formation

Samples	Opaque Minerals	Non-Opaque Minerals				TNOP	Z %	T %	R %	O %	ZTR index	[45]
		Z	T	R	O							
BID1	120	13	50	24	75	162	8.02	30.86	14.81	46.30	53.70	Mature
BID2	225	17	84	74	59	234	7.26	35.90	31.62	25.21	74.79	Mature
BID3	190	16	39	35	90	180	8.89	21.67	19.44	50.00	50.00	Mature
BID4	249	23	84	44	45	196	11.73	42.86	22.45	22.96	77.04	Super-mature
BID5	280	19	40	42	84	185	10.27	21.62	22.70	45.41	54.59	Mature
BID6	265	25	52	20	70	167	14.97	31.14	11.98	41.92	58.08	Mature
BID7	290	45	120	85	77	327	13.76	36.70	25.99	23.55	76.45	Super-mature
BID8	274	20	53	13	65	151	13.25	35.10	8.61	43.05	56.95	Mature
BID9	361	17	190	109	86	402	4.23	47.26	27.11	21.39	78.61	Super-mature
BID10	105	23	95	65	55	238	9.66	39.92	27.31	23.11	76.89	Super-mature

DOI: https://doi.org/10.53704/fujnas.v14i2.970

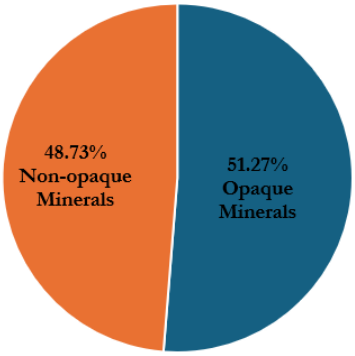

Fig. 14: Pie chart showing percentages of opaque and non-opaque minerals of the sandstone studied

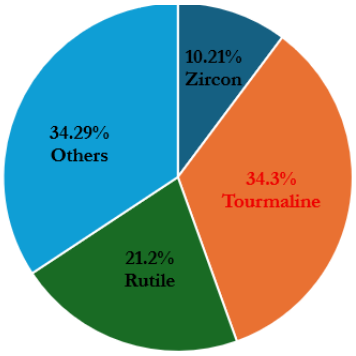

Fig. 15: Pie Chart showing the percentage of non-opaque minerals in the Bida sandstone

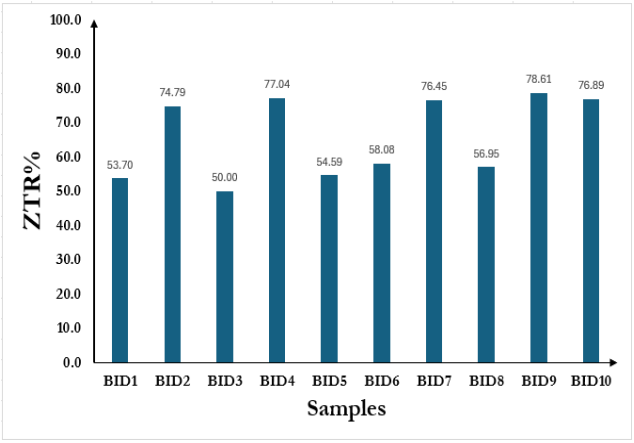

Fig. 16: Bar Chart of ZTR index of each selected sample of Bida Sandstone

The heavy mineral analysis suggests that the sediments are predominantly highly mature and primarily sourced from the erosion of felsic igneous (granitic) and high-grade metamorphic rocks. The consistently high ZTR values, particularly the "super-mature" classification observed in several samples, indicate that sediment recycling from older, well-matured sedimentary units likely plays a major role in the provenance of these samples.

Conclusions

The study employs grain-size analysis to interpret the palaeodepositional environment at selected locations in the Bida Basin. Using statistical grain size parameters, the research characterises depositional processes, sediment transport, and hydrodynamic conditions. The findings reveal that the sandstones are predominantly medium- to coarse-grained, moderately to poorly sorted, and exhibit varied skewness and kurtosis. These characteristics suggest fluctuations in energy levels and sediment sources. Bivariate plots indicate a primarily fluvial origin with some coastal and marine influences. The study concludes that the dominance of medium- to coarse-grained sandstones, coupled with moderate to poor sorting, suggests good reservoir potential with adequate porosity and permeability. The prevalence of beach and fluvial deposits supports enhanced reservoir connectivity and hydrocarbon migration pathways, while shallow marine sediments may provide effective trapping mechanisms. The interplay of fluvial and turbidity deposits highlights the potential for stratigraphic traps, which are crucial for hydrocarbon exploration.

Petrographic analysis reveals a predominance of quartz, indicating a mature sediment source likely originating from cratonic or recycled orogenic terrains, where extensive weathering and transport have led to the breakdown of feldspars. The presence of various non-opaque minerals suggests a mixed provenance, with input from multiple source regions. Additionally, a high ZTR index indicates a mature to supermature sediment stage. Among the study locations, Kutigi and Bida exhibit the most favourable conditions for hydrocarbon storage, owing to their well-sorted grains and more uniform distribution, which enhance permeability. In contrast, other areas may require secondary porosity mechanisms, such as fracturing, to improve reservoir quality. The study concludes that Kutigi and Bida, with their well-sorted, high-energy depositional environments, are promising zones for hydrocarbon accumulation and migration. Although less prevalent, shallow marine sediments in the area could also contribute as hydrocarbon traps.

Competing interest statements

Regarding the subject matter of this research, the authors have no conflicts of interest to disclose.

DOI: https://doi.org/10.53704/fujnas.v14i2.970

References

1. Folk, R.L. & Ward, M.C., (1957). Brazos River bars: a study in the significance of grain Size parameters. Journal of Sedimentary Research 27, 3–27.
2. Friedman, G.M., (1961). Distinction between dunes, beaches, and river sands from their Textural Characteristics. Journal of Sedimentary Research 31, 514–529.
3. Friedman, G.M., (1967). Dynamic processes and statistical parameters compared for the Size-frequency distribution of beach river sands. Journal of Sedimentary Research 37, 327–354.
4. Griffiths, J.C., (1967). Scientific methods in the analysis of sediments. McGraw-Hill, New York, 508 pp.
5. Sahu, B.K., (1964). Depositional mechanisms from the size analysis of clastic sediments. Journal of Sedimentary Research 34, 73–83.
6. Sahu, B.K., (1983). Multi-group discrimination of depositional environments using size Distribution Statistics. Indian Journal of Earth Science 10, 20–29.
7. Ghosh, S.K. & Chatterjee, B.K., (1994). Depositional mechanisms as revealed from grain-Size measures of the palaeo-proterozoic Kolhan siliciclastics, Keonjhar District, Orissa, India. Sedimentary Geology 89, 181–196.
8. Tripathi, A. & Hota, R.N., (2013). Granulometric Analysis of Ib River Sediments near Sundargarh, Odisha.
9. Kanhaiya, S. & Singh, B.P., (2014). Spatial variation of textural parameters in a small river: An example from Khurar River, Khajuraho, Chhaterpur District, Madhya Pradesh, India. Global Journal of Earth Science and Engineering 1, 34–42.
10. Ahmad, F., Quasim, M.A., Ghaznavi, A.A., Khan, Z. & Ahmad, A.H.M., (2017). Depositional Environment as revealed from lithofacies and grain size Measures of the Jurassic Fort Member rocks, Jaisalmer Formation, western Rajasthan. Geologica Acta 15, 153–167.
11. Kanhaiya, S., Singh, B.P. & Srivastava, V.K., (2017). Surface textures of detrital quartz grains derived from Bun delkhand granite in the Khurar River, central India. Vietnam: Geo-spatial technology and Earth resources. Publishing House for Science and Technology, 575–581.
12. Hartmann, D., (2007). From reality to model: operationalism and the value chain of Particle size analysis of natural sediments. Sedimentary Geology 202, 383–401.
13. Weltje, G.J. & Prins, M.A., (2007). Genetically meaningful decomposition of grain-size distributions. Sedimentary Geology 202, 409–424.
14. Cheetham, M.D., Keene, A.F., Bush, R.T., Sullivan, L.A. & Erskine, W.D., (2008). A Comparison of grain-size analysis methods for sand-dominated fluvial sediments. Sedimentology 55, 1905–1913.
15. Srivastava, A.K. & Mankar, R.S., (2008). Grain size analysis and depositional pattern of Upper Gondwana sediments (Early Cretaceous) of Svalbard area, districts Amravati, Maharashtra, and Betul, Madhya Pradesh. Journal of Geological Society of India 73, 393–406.
16. Reading, H.G., (1996). Sedimentary Environments: Processes, Facies and Stratigraphy. 3rd Edition, Blackwell, Oxford, 689 pp.
17. Falconer, J.D., (1911). The Geology and Geography of Northern Nigeria. Macmillian, London, 255 pp.
18. Russ, W., 1930. The Minna-Birnin Gwarri belt: reports of the Geological Survey of Nigeria, pp. 10–14.
19. Jones, H.A., (1958). The oolitic ironstone of Agbaja Plateau, Kabba Province. Record of the Geological Survey of Nigeria, 20–43.
20. Adeleye, D.R., Dessauvagie, T.F.J., (1972). Stratigraphy of the Niger embayment, near Bida, Nigeria. In: Dessauvagie, T.F.J., Whiteman, A.J. (Eds.), African Geology. University of Ibadan Press, pp. 181–186. https://doi.org/10.1016/j.heliyon.2021.e07205.
21. Jan du Chene, R.E., Adegoke, O.S., Adediran, S.A., Petters, S.W., (1978). Palynology and foraminifera of the Lokoja Sandstone (Maastrichtian), Bida Basin, Nigeria. Revista Espanola de Micropaleontotologia 10, 379–393.
22. Idowu, J.O., Enu, E.I., (1992). Petroleum geochemistry of some late Cretaceous shale from the Lokoja Sandstone of the Middle Niger Basin, Nigeria. Journal of African Earth Sciences 14, 443–455.
23. Ojo, OJ, Akande, SO, (2003). Facies relationships and depositional environments of the Upper Cretaceous Lokoja Formation in the Bida Basin, Nigeria. J. Min. Geol. 39, 39–48. https://doi.org/10.30564/agger.v4i3.4933.
24. Akande, S.O., Ojo, O.J., Erdtmann, B.D., Hetenyi, M., (2005). Paleoenvironments, Organic petrology and Rock-Eval studies on source rock facies of the Lower Maastrichtian Patti Formation, Southern Bida Basin, Nigeria. J. Afr. Earth Sci. 41, 394–406.
25. Agyingi, CM, (1991). Geology of Upper Cretaceous Rocks in the Eastern Bida Basin, Central Nigeria. University of Ibadan, Nigeria, p. 501.
26. Braide, S.P., (1992). Geological development, origin, and energy mineral resources Potential of the Lokoja Formation in the southern Bida Basin. Journal of Mining and Geology 28, 33–44.
27. Ladipo, K.O., Akande, S.O., Mucke, A., (1994). Genesis of ironstone from middle Niger Sedimentary Basin, evidence from sedimentology, ore microscope, and geochemical studies. Journal of Mining and Geology 30, 161–168.
28. Mücke, A, Badejoko, TA, Akande, SO, (1999). Petrographic-microchemical studies and the origin of the Agbaja Phanerozoic Ironstone Formation, Nupe Basin, Nigeria: a product of a ferruginized ooidal kaolin precursor not identical to the Minette type. Mineralium Deposita 34, 284–296.
29. Folk, R.L. & Ward, M.C., (1957). Brazos River bars: a study in the significance of grain Size parameters. Journal of Sedimentary Research 27, 3–27.
30. Olawoki, O. A., & Nwachukwu, J. I. (2018). *The Prospectivity and Exploration Potential of Onshore Slope Fan Play, Niger Delta Basin, Nigeria*. International Journal of Geology & Earth Sciences, 4(3), 10–22. https://doi.org/10.32937/IJGES.4.3.2018.10-22
31. Dickinson WR (1970). Interpreting provenance relations from detrital modes of sandstones. In: Zuffa G. G (ed.) Provenance of Arenites. Riedel, Dordrecht, NATO Advanced study Institute Series 148:333-361.
32. Sutherland, R.A. & Lee, C.T., (1994). Discrimination between coastal sub environments using textural characteristics. Sedimentology 41, 1133–1145.
33. Folk, R.L. (1980). Petrology of Sedimentary Rocks. Hemphill, Austin, 182 pp.
34. Boggs, S. (1995). Principles of Sedimentology and Stratigraphy (2nd ed.). Prentice Hall, Englewood Cliffs, NJ.

DOI: https://doi.org/10.53704/fujnas.v14i2.970

35. Boggs, S.Jr. (2009). Petrology of Sedimentary Rocks, Second Edition, Cambridge University Press, New York, 67 98 pp.
36. Al-Juboury, A. I. (1994). Petrology and provenance of the Upper Fars Formation (Upper Miocene), Northern Iraq. Acta Geologica Universitatis Comenianae Bratislava, 50, 45–53.
37. Tucker, ME, (1985). Sedimentary Petrology: An Introduction. Blackwell Scientific Publications, p. 252.
38. Selley, RC (1985). Ancient Sedimentary Environment. Cornell University Press, Ithaca, New York, p. 317
39. Fang, S., Guo, Z., Zhang, Z., & Wu, C. (2004). *Discussion on Mesozoic–Cenozoic Evolution of Tian Shan and Its Adjacent Basins*. Acta Scientiarum Naturalium Universitatis Pekinensis, 40(6), 886–895.
40. Ruiz, G. M. H., Seward, D., & Winkler, W. (2007). Evolution of the Amazon Basin in Ecuador with special reference to hinterland tectonics: data from zircon fission-track and heavy mineral analysis. In: Heavy Minerals in Use, Developments in Sedimentology, Vol. 58, pp. 907–934. Elsevier.
41. Tucker, ME, (1988). Sedimentary Petrology: An Introduction. Blackwell Scientific Publications, p. 252.
42. Elyas, Yasin Khalil (1988). *Tourmalinisation in the Cheviot Granite*. M.Phil. Thesis, University of Newcastle upon Tyne.
43. Pettijohn F. J., (1975). Sedimentary rocks, 3rd ed. New York: Harper and Row.
44. Kern, D. Q., and Seaton, R. E. (1959). *A theoretical analysis of thermal surface fouling*. British Chemical Engineering, 4(5), 258–262.
45. Hubert, J. T. (1962). Zircon-tourmaline-rutile maturity index and interdependence of the composition of heavy minerals assemblages with the gross composition and texture of sandstones. J. Sed pet. v.. 32, p 440-450.

DOI: https://doi.org/10.53704/fujnas.v14i2.970